Human Based Cost from Persistent Homology for Bipedal Walking

Ram Vasudevan*, Aaron D. Ames, and Ruzena Bajcsy***

** Electrical Engineering and Computer Sciences*
University of California, Berkeley
Berkeley, CA 94720
{ramv,bajcsy}@eecs.berkeley.edu

*** Mechanical Engineering*
Texas A&M University
College Station, TX 77843
aames@tamu.edu

Abstract: While the focus of robotic bipedal walking to date has been the development of anthropomorphic gait, the community has been unable to agree on a model for such gait. In this paper, we propose a *universal* ordering of events for bipedal walking based on motion capture data collected from a walking experiment. We process the motion capture data using persistent homology to automatically determine the ordering of discrete events. Surprisingly, every subject in the experiment had an *identical* ordering of such events. This universal ordering allows us to propose a cost function based upon human data: *the human-based cost*.

1. INTRODUCTION

The goal of bipedal walking is typically not to minimize a concrete cost, like torque squared or the specific cost of transport, but rather to achieve the more ambitious goal of obtaining human-like walking. The design of a controller to achieve this objective is implicitly related to the discrete ordering of events, *domain breakdown*, i.e. the sequence of constraints enforced during walking. For the specific discrete ordering of events illustrated in Fig. 1 knowing that a controller must ensure that a transition occurs from the left toe domain, denoted $[lt]$, to the left toe and right heel domain, denoted $[lt, rh]$, is inherently connected with the domain breakdown. In fact, in a recent paper we showed that the temporal ordering of discrete events along with a Lagrangian model, which is purely a function of the mechanical design of the robot, completely determines the mathematical model of a biped Ames et al. (2011).

Given the importance of the domain breakdown for bipedal robotic walking, one would suspect that in fact there existed some consensus on the ordering of discrete modes. Unfortunately, the history of robotic walking is riddled with uncertainty on the appropriate domain breakdown. Traditional models of bipedal robots have for simplicity employed a single domain model (Ames et al. (2007); Goswami et al. (1996); Tedrake et al. (2005); Westervelt et al. (2007)), since it assumes an instantaneous double support phase and excludes the presence of feet. Adding feet to the bipedal robot requires the extension of the domain breakdown beyond a single discrete phase and is typically done by either adding a phase where the heel is off the ground or a double support phase where both feet are on the ground, or any combination thereof Choi and Grizzle (2005); Schaub et al. (2009); Tlalolini et al. (2009). This lack of consistency among models demands the question of if there does in fact exist a single "universal" domain breakdown to achieve anthropomorphic walking. Implicit in this question is the desire to quantify how human-like a certain domain breakdown truly is.

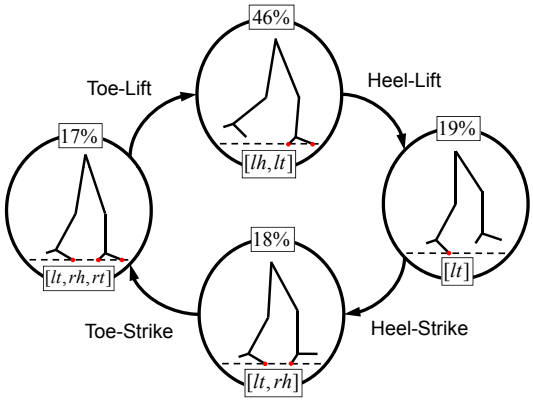

Fig. 1. An example of a *domain breakdown*, where the red dots indicate the constraints enforced in each domain.

The goal of this paper is two-fold: first to determine a universal anthropomorphic domain breakdown for bipedal walking and second to employ this breakdown to construct a *human-based cost* that measures the anthropomorphism of a gait. Our contributions are as follows. First, in Section 3, we develop a motion capture dataset that we make available of nine healthy diverse people walking in a straight line. Second, in Section 4, we develop a novel procedure exploiting persistent homology to determine constraint enforcement and hence a domain breakdown and show that every subject in our experiment has an *identical* domain breakdown illustrated in Fig. 1. Third, in Section 5, we show that by considering a metric over weighted graphs we can develop a cost function that measures how human-like a gait is. The paper includes a discussion of notation in Section 2 and a conclusion in Section 6.

2. FROM CONSTRAINTS TO MODELS

Bipeds evolve in a continuous fashion according to traditional equations of motion when a fixed number of points of the biped are in contact with the ground, e.g., when one foot is flat on the ground while the other swings for-

ward. The discrete behavior in the system occurs when the number of contact points change. Since our previous work showed how to construct a hybrid system model of a biped using the intrinsic equations of motions of a biped and the temporal ordering of constraints Ames et al. (2011), in this section we introduce the notation required to go from the temporal ordering of constraints to a domain breakdown.

Graphs and Cycles. A graph is a tuple $\Gamma = (V, E)$, where V is the set of vertices and $E \subset V \times V$ is the set of edges; an edge $e \in E$ can be written as $e = (i, j)$, and the source of e is source$(e) = i$ and the target of e is target$(e) = j$. Since steady state bipedal walking naturally appears periodic, we are interested in hybrid systems *on a cycle* and are therefore interested in graphs that contain cycles or are themselves cycles. A *directed cycle* (or just a cycle) is a graph $\ell = (V, E)$ such that the edges and vertices can be written as:

$$V = \{v_0, v_1, \dots, v_{p-1}\}, \quad (1)$$
$$E = \{e_0 = (v_0, v_1), \dots, e_{p-1} = (v_{p-1}, v_0)\}.$$

Since in the case of a cycle, the edges are completely determined by the vertices, we sometimes simply denote a cycle by:

$$\ell : v_0 \to v_1 \to \cdots \to v_{p-1}.$$

In the case when a graph Γ is being considered with more than one cycle, we denote a cycle in the graph by $\ell \subset \Gamma$.

Example 1. The domain graph pictured in Fig. 1 is a directed cycle: $\Gamma_u = (V_u, E_u)$. There are 4 vertices and edges, which results in the cycle:

$$\ell_u : [lh, lt] \to [lt] \to [lt, rh] \to [lt, rh, rt].$$

Constraints. The continuous dynamics of the system depend on which constraints are enforced at any given time, while the discrete dynamics depend on the change in constraints. Constraints and their enforcement are dictated by the number of contact points of the system with the ground. Specifically, we define the *set of contact points* as set $\mathcal{C} = \{c_1, c_2, \dots, c_k\}$, where each c_i is a specific type of contact possible in the biped, either with the ground or in the biped itself (such as the knee locking). There are four contact points of interest given by:

$$\mathcal{C} = \{lh, lt, rh, rt\}$$

where lh and lt indicate the left heel and toe, and rh and rt indicate right heel and toe, respectively. Contact points introduce *holonomic constraints* on the system that must be held constant for the contact point to be maintained.

Domain Breakdowns. A domain breakdown is a directed cycle together with a specific choice of contact points on every vertex of that graph. To define this formally, we assign to each vertex a binary vector describing which contact points are in force on that domain.

Definition 1. Let Γ be a directed cycle and $\mathcal{C} = \{c_1, c_2, \dots, c_k\}$ a set of contact points. A *domain breakdown* is is a function $\mathcal{B} : V \to \mathbb{Z}_2^k$ such that $B(v)_i = 1$ if c_i is in contact on v and $B(v)_i = 0$ otherwise.

Example 2. In the case of the graph Γ_u given in Example 1 and set of contact points $\mathcal{C} = \{lh, lt, rh, rt\}$, for the domain breakdown given in Fig. 1, this domain breakdown is formally given by $\mathcal{B}_u : V_u \to \mathbb{Z}_2^4$ where $\mathcal{B}_u(hl) = [1, 1, 0, 0]^T$, $\mathcal{B}_u(hs) = [0, 1, 0, 0]^T$, $\mathcal{B}_u(ts) = [0, 1, 1, 0]^T$ and $\mathcal{B}_u(tl) = [0, 1, 1, 1]^T$. Note that in this case the choice of "left" and "right" leg is arbitrary, as long as it is kept consistent throughout the definition. The terms stance and non-stance leg are often used in the literature as well, but with the existence of double support phases this choice also becomes arbitrary.

Given the importance of the domain breakdown in determining the hybrid model of a biped, part of the goal of this paper is to determine whether there exists a common domain breakdown for all humans.

3. EXPERIMENTAL SETUP

In this section, we describe the experimental setup employed during data collection and describe the preprocessing done before determining the domain breakdown for each individual. After reading the description presented in this section, any interested researcher should be able to perform analysis on the collected data [1].

The data presented in this paper is collected using the Phase Space System [2], which computes the 3D position of LED sensors at 480 frames per second using 6 cameras. The cameras were calibrated prior to the experiment and were placed to achieve a 1 millimeter level of accuracy for a space of size 4 by 4 by 4 meters cubed. In addition to the LED sensors placed as in Fig. 2, 1 LED sensor was placed on the sternum, 1 LED sensor was placed on the back behind the sternum, and 1 LED sensor was placed on the belly button. Each sensor was fastened to subjects in a manner that ensured that they did not move during the experiment. Each trial of the experiment required the subject to walk 3 meters along a line drawn on the floor. To simplify the data analysis each subject was required to place their right foot at the starting point of the line at the outset of the experiment and was told to walk

[1] The collected data can be found at `http://www.eecs.berkeley.edu/~ramv/HybridWalker.html`

[2] `http://www.phasespace.com/hardware.html`

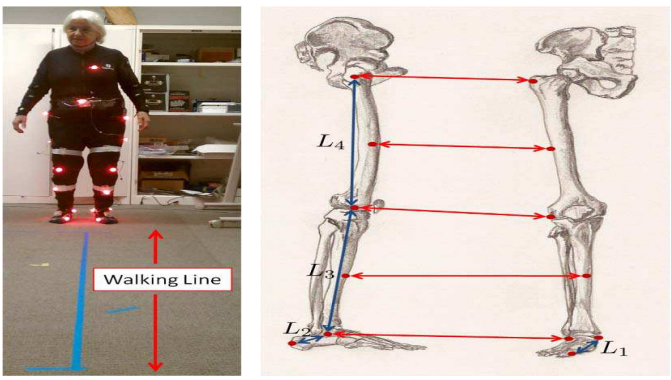

Fig. 2. Illustration of the experimental setup (left) and sensor placement on each leg (right). Each subject in the experiment was required to wear a suit with sensors colored in red. Each sensor was placed at the joints as illustrated with the red dots on the lateral and anterior aspects (right) of the right leg. The same sensors drawn from different views are connected with red arrows.

	Sex	Age	Weight	Height	L_1	L_2	L_3	L_4
1	M	30	90.7	184	14.5	8.50	43.0	44.0
2	F	19	53.5	164	15.0	8.00	41.0	44.0
3	M	17	83.9	189	16.5	8.00	45.5	55.5
4	M	22	90.7	170	14.5	9.00	43.0	39.0
5	M	30	68.9	170	15.0	8.00	43.0	43.0
6	M	29	59.8	161	14.0	8.50	37.0	40.0
7	M	26	58.9	164	14.0	9.00	39.0	41.0
8	F	77	63.5	163	14.0	8.00	40.0	42.0
9	F	23	47.6	165	15.0	8.00	45.0	43.0

Fig. 3. Table describing each of the subjects. The measurements in column 4 are in kgs and the measurements in columns $5-9$ are in cms. The labels in columns $6-9$ correspond to those illustrated in Fig. 2.

in a natural manner. Each subject performed 12 trials, which constituted a single experiment. Fig. 3 describes the measurements of each of the subjects.

To make the data collected from walking experiment amenable to analysis, it was processed through a three-step procedure: interpolation, data rotation and averaging. Since the motion capture information drops out periodically due to self-occlusions, we first interpolate the data to compensate for sensors dropping out of contact with the camera. From each of the trials, at least two steps are isolated (one with the right leg and another with the left leg) by ensuring that the data repeats. The data is then rotated so that the walking occurs in the x-direction. Since we are only interested in the data corresponding to constraint enforcement, only the sensor data for the heel and toe on each leg are considered (this is shown in Fig.4(a)). For each subject, this data is considered for all 12 walking trials and averaged (after appropriately shifting the data in time) which results in a single trajectory for each constraint for each subject for at least two steps (one step per leg); this is the data that is used to determine the domain breakdown and is drawn in Fig.4(b).

4. DOMAIN BREAKDOWN

In this section, we present our approach to determining when and which constraints are enforced through the course of a step. Doing so allows for a temporal ordering of events, yielding a domain breakdown. This would appear to be a simple task—for example, in the case of the heel, one need only determine when it is or is not on the ground—but this turns out to be non-trivial.

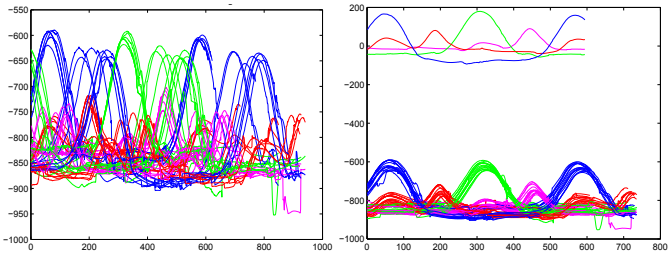

(a) Original Data (b) Postprocessed Data

Fig. 4. (a) The data for the height (in mm) of the heel and toe for each leg for all 12 trials of a single individual and (b) the data after it has been shifted (drawn at the bottom of the plot) and averaged (drawn at the top of the plot after it has been shifted to have zero mean). Each color corresponds to a different sensor.

The obvious approach to determining the domain breakdown based upon the human data is to threshold the data, i.e., below the threshold a given constraint (heel or toe) is enforced and above it, it is not. Due to the noisy nature of the data for the constraints "near the ground," choosing a proper threshold occurs at the scale of the noise. Smoothing the data aggressively can "essentially" solve this problem, but then there becomes too many subject specific defined parameters in the domain fitting, i.e. the degree of smoothing and the threshold. It is desirable to, instead, have a domain breakdown that is chosen "automatically," i.e., a domain breakdown that is independent of choices on thresholds and other parameters. To overcome this problem, we employ the notion of persistent homology which was introduced by Carlsson et al. (2004).

4.1 Persistent Homology

We begin by defining simplicial complexes and homology. The reader is encouraged to read Hatcher (2002) for a more complete introduction.

Definition 2. A **simplicial complex** is a set K, together with a collection Ω of subsets of K called **simplices** such that for all $v \in K$, $\{v\} \in \Omega$, and if $\sigma \subseteq \omega \in \Omega$, then $\sigma \in \Omega$. We call the sets $\{v\}$ the **vertices** of K.

Definition 3. We say $\omega \in \Omega$ is a **k-simplex of dimension k** if $|\omega| = k+1$ where $|\omega|$ denotes the cardinality of the set ω. An **orientation** of a k-simplex $\omega = \{v_0, \ldots, v_k\}$, is an equivalence class of orderings of the vertices of ω, where $\{v_0, \ldots, v_k\} \sim \{v_{\tau(0)}, \ldots, v_{\tau(k)}\}$. We denote an oriented simplex by (ω).

Definition 4. The **kth chain group** C_k of K is the free Abelian group on its set of oriented k-simplices. An element $c \in C_k$ is a k-chain, $c = \sum_i n_i(\omega_i)$, $\omega \in K$ with coefficients $n_i \in \mathbb{Z}$.

Homology provides a means for an algebraic description of each simplicial complex.

Definition 5. The **boundary operator** $\partial_k : C_k \to C_{k-1}$ is a homomorphism defined linearly on a chain $c \in C_k$ by its action on any simplex $\omega = (v_0, v_1, \ldots, v_k) \in c$, $\partial_k \omega = \sum_i (-1)^i (v_0, v_1, \ldots, \hat{v_i}, \ldots, v_k)$, where $\hat{v_i}$ indicates that v_i is deleted from the sequence. The boundary operator connects the chain groups into a **chain complex** C_*. We may also define subgroups of C_k using the boundary operator: the **cycle group** $Z_k = \ker \partial_k$, and the **boundary group** $B_k = \text{im } \partial_{k+1}$ The k**-th homology group** is the quotient group $H_k := Z_k / B_k$. The **homology** of a complex is the collection of all homology groups. The rank of H_k is the k**-th Betti number** β_k.

The Betti numbers of a chain group carry an important topological meaning. β_0 is equal to the number of connected components in a chain group and β_k for $k > 0$ is equal to the number of k-dimensional holes in a chain group. The Betti numbers in a topological sense fully characterize a simplicial complex since they are preserved under continuous deformation. Suppose we now construct a simplicial complex by thresholding an image over its

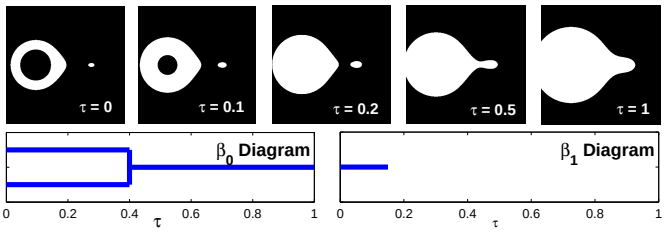

Fig. 5. The collection of thresholded images (top) start with two connected components which merge at $\tau = 0.4$ as shown in the β_0 diagram. A hole is present until $\tau = 0.15$ as depicted in the β_1 diagram.

intensity values and treating each pixel in the image as a node in the complex. Edges between nodes would arise when neighboring pixels in the thresholded image shared the same intensity value. An example of the application of this procedure to an image as a function of a threshold, τ, can be found in Fig. 5.

It is possible to track the Betti numbers as a function of the parameter τ. This information is depicted as a persistence diagram at the bottom of Fig. 5. Notice that for any threshold greater than $\tau = 0.4$ corresponds to the most *persistent* topologically identical description of the image (i.e. the number of connected components and the number of holes are unchanged by choosing any larger threshold). We employ the sensor data to construct a simplicial representation as a function of a threshold for the contact constraints that are enforced and search for the threshold corresponding to the most persistent topological description of the data.

4.2 Determining the Domain Breakdown

We now describe how given a set of distinct thresholds for each motion capture sensor we construct a simplicial complex. Let the two toe and two heel sensors time series

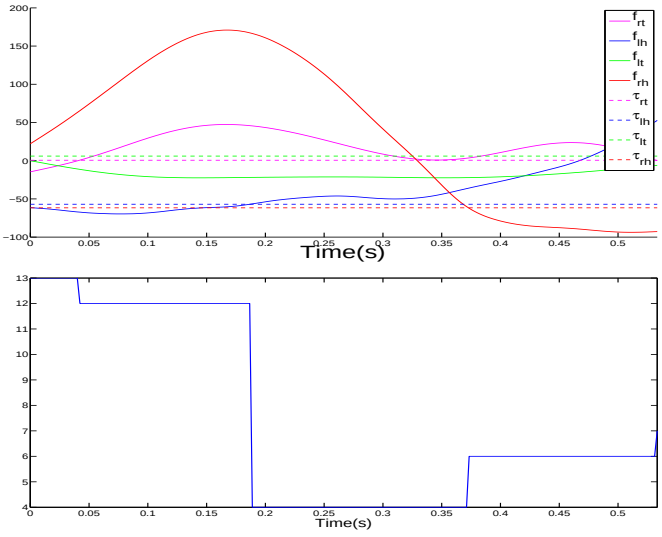

Fig. 6. An illustration of the procedure to construct a simplicial complex from motion capture sensor data (top) via $C(\cdot, t)$ (bottom) where we have transformed each combination of contact points, from $\mathbb{Z}_2^4$ to its decimal expansion.

data be denoted as f_{lh},f_{lt},f_{rt},f_{rh} : $[0, T] \to \mathbb{R}$. Given a set of thresholds for each sensor, $\tau \equiv (\tau_{lh},\tau_{lt},\tau_{rh},\tau_{rt})$, and encoding each combination of contact points as an element of $\mathbb{Z}_2^4$ (as we did in Example 2), we can define a function, $C : \mathbb{R}^4 \times [0, T] \to \mathbb{Z}_2^4$, which describes which set of constraints is active at a given time:

$$C(\tau, t; f_{lh}, f_{lt}, f_{rt}, f_{rh}) = \begin{bmatrix} \mathbb{1}\{f_{lh}(t) < \tau_{lh}\} \\ \mathbb{1}\{f_{lt}(t) < \tau_{lt}\} \\ \mathbb{1}\{f_{rh}(t) < \tau_{rh}\} \\ \mathbb{1}\{f_{rt}(t) < \tau_{rt}\} \end{bmatrix}. \quad (2)$$

Fig. 6 illustrates C for a given threshold. Given this function and a threshold, τ we can define a simplicial complex, Ω^τ. The $0-$simplices of Ω^τ correspond to all combinations of contact points (i.e. we would have sixteen $0-$simplices). The $1-$simplices of Ω^τ correspond to transitions within the function C. That is, if $C(\cdot, t^-) = v_1$ and $C(\cdot, t^+) = v_2$ where $v_1 \neq v_2$, then we include the $1-$simplex $\{v_1, v_2\}$ in Ω^τ. For the illustration in Fig. 6 the $1-$simplices in Ω^τ are $\{[lh, lt], [lt]\}$,$\{[lt], [lt, rh]\}$,$\{[lt, rh], [lt, rh, rt]\}$.

As we described earlier, we can compute the Betti numbers for each of these simplicial complex, Ω^τ.We employ the persistence homology argument to search over the space of thresholds to find the most topologically persistent domain breakdown (i.e. the threshold which corresponds to the most persistent number of connected components and cycles) and treat this as the domain graph corresponding to the walker. Some care must be taken in choosing an interval of interest over which to perform the thresholding. Since the subjects performed a walking experiment, at any instance at least one toe constraint was active and at least once each toe constraint was inactive which allows us to immediately restrict the space of thresholds for each toe over which to perform the analysis. Similarly each heel constraint was active and inactive at least once during the experiment allowing us to restrict the space of thresholds for each heel.

After performing the aforementioned procedure, we consider the domain breakdowns for the various subjects. We notice as illustrated in Fig. 7 that in spite of the vast differences in age, height, and weight all subjects exhibit the *universal* domain breakdown shown in Fig. 1. This is particularly surprising, since we made no *a priori* assumptions about the ordering of constraint enforcement and did not demand simultaneous constraint enforcement between legs.

5. COST OF WALKING FROM HUMAN DATA

In this section, we construct a cost function that measures the anthropomorphic nature of robotic bipedal walking termed the *human-based cost*. We do this by first defining a metric on the space of weighted cycles, the *cut distance*, which allows us to compare different walking gaits and to construct an optimal walking cycle by minimizing the distance between the weighted cycles observed in the human walking data. Using the cut distance, we next define the *human-based cost* which allows us to compute the distance from a specific walking gait (either human or robotic) to the optimal walking cycle. The remainder of this section is devoted to using the human-based cost

to determine the extent to which popular robotic models from the literature are anthropomorphic.

Distance Between Cycles. We employ the notion of *cut* (or *rectangular*) distance between two weighted graphs to compare different domain breakdowns (the definition in its general form can be found in Borgs et al. (2008)). Since we are only interested in the specific domains visited and the corresponding time spent in each of these domains, we define a notion of weighted cycle and a corresponding distance between weighted cycles that is pertinent to the application being considered.

Definition 6. A *walking cycle* is a pair (α, ℓ) where $\ell = (V, E)$ is a cycle and $\alpha : \ell \to \mathbb{R}^{|V|}$ is a function such that $\alpha(v) \geq 0$ and $\sum_{v \in V} \alpha(v) = 1$. Denoting a cycle by $\ell : v_0 \to v_1 \to \cdots \to v_p$, we denote a walking cycle by:

$$\alpha(\ell) : \alpha(v_0) \to \alpha(v_1) \to \cdots \to \alpha(v_p).$$

Example 3. Each of the domain breakdowns presented in Fig. 7 has a distinct walking cycle. For example, Subject 1 has a walking cycle $S_1 = (\alpha_1, \ell_1)$ given by:

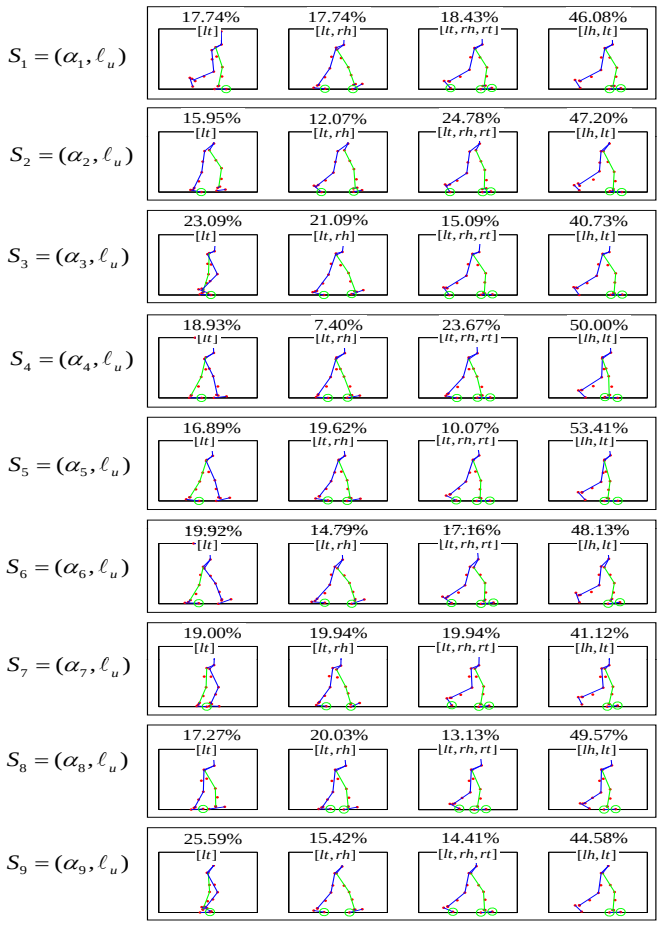

Fig. 7. The domain breakdowns in each row for the 9 subjects in the order listed in Fig. 3 participating in the experiment. Comparing with the hybrid system illustrated in Fig. 1 the first through fourth rows correspond to $[lh, lt]$, $[lt]$, $[lt, rh]$, and $[lt, rh, rt]$, respectively. Each illustration is a snapshot of the subject in the domain and above each plot is the percentage of the total gait spent in that domain.

$$\begin{array}{rccccc} \ell_1 : & [lt] & \to & [lt, rh] & \to & [lt, rh, rt] \to [lh, lt] \\ \alpha_1(\ell_1) : & 17.74\% & \to & 17.74\% & \to & 18.43\% \to 46.08\%. \end{array}$$

Weightings are stated in percentages to indicate the physical quantity that they represent: the time the human spends in a domain through the course of one step.

We now introduce a definition of cut distance that is a slight modification of the definition presented in Borgs et al. (2008). The only differences are that we do not force the weighted graphs to have nodes with positive weights, and we require the weights to sum to one.

Definition 7. Let (α_1, ℓ_1) and (α_2, ℓ_2) be two walking cycles. Viewing both α_1 and α_2 as functions on $V_1 \cup V_2$ by letting $\alpha_1(i) \equiv 0$ if $i \in V_2 \backslash V_1$ and $\alpha_2(j) \equiv 0$ if $j \in V_1 \backslash V_2$, the *cut distance between two cycles* is given by:

$$d(\alpha_1, \ell_1, \alpha_2, \ell_2) = \sum_{k \in V_1 \cup V_2} |\alpha_1(k) - \alpha_2(k)| +$$

$$\max_{I, J \subset V_1 \cup V_2} \left| \sum_{i \in I, j \in J} (\alpha_1(i)\alpha_1(j)\beta_1(i,j) - \alpha_2(i)\alpha_2(j)\beta_2(i,j)) \right|$$

where $\beta_1(i,j) = 1$ for all edges $(i,j) \in E_1$ and $\beta_2(i,j) = 1$ for all edges $(i,j) \in E_2$.

It is straightforward to check that the modified cut distance satisfies the requirements of a metric (i.e. non-negativity, identity of indiscernibles, symmetry and the triangle inequality). Intuitively, the cut distance compares just how different two walking cycles are when considering all possible "cuts" between the pair of cycles.

Human-Based Cost. In the context of this paper, we develop a cost based upon the domain breakdown and resulting walking cycles to determine how anthropomorphic a gait is.

Definition 8. Consider N subjects with associated domain breakdowns and walking cycles $S_i = (\alpha_i, \ell_i)$ for $i \in \{1, \ldots, N\}$. Letting $\mathscr{L} = \bigcup_{i=1}^{N} \ell_i$ be the graph obtained by combining all of the cycles ℓ_i, we define the *optimal walking cycle* by:

$$(\alpha^*, \ell^*) = \underset{(\alpha, \ell) \in \mathbb{R}^{|\ell|} \times \mathscr{L}}{\operatorname{argmin}} \frac{1}{N} \sum_{i=1}^{N} d(\alpha, \ell, \alpha_i, \ell_i). \tag{3}$$

The optimal walking cycle is just the walking cycle through the graph of all cycles obtained from the walking that best fits the data under the cut distance. The optimal walking cycle allows one to describe the extent to which a walking gait is human-like.

Definition 9. Given a biped (either human or bipedal robot) with associated domain breakdown and walking cycle $R = (\alpha_r, \ell_r)$, the *human-based cost (HBC) of walking* is defined to be:

$$\mathcal{H}(R) = d(\alpha_r, \ell_r, \alpha^*, \ell^*).$$

It is important to note that the optimal walking cycle may not be unique, and so there may be multiple HBCs of walking constructed from a single experiment, i.e., the HBC is not necessarily unique (in this paper, we found a unique HBC). Unsurprisingly, multiple experiments might yield different HBCs, but if the experiments are carried out consistently they should be compatible.

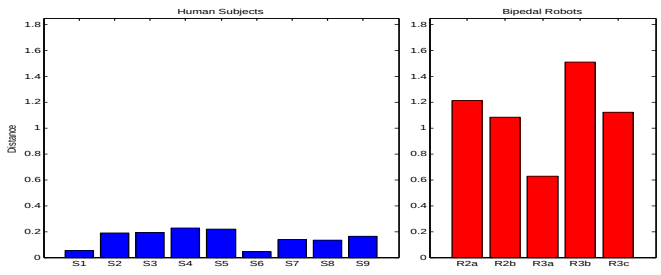

Fig. 8. The HBC for the 9 subjects in the experiment (left), 5 bipedal robotic models that have appeared in the literature (right, with the number of domains in each of the models is illustrated by subscripts).

Next, we consider the domain breakdowns for the 9 subjects in the walking experiment. Since there is a unique cycle, it is unsurprising that there is a unique optimal walking cycle and therefore unique HBC. Using the walking cycles illustrated in Fig. 7, we now compute the optimal walking cycle and compute the HBC for the subjects and bipedal robots that have appeared in the literature. All the subjects have the same universal cycle ℓ_u and so $S_i = (\alpha_i, \ell_u)$ for $i = 1, \ldots, 9$ and the optimal walking cycle is given by (α^*, ℓ_u), where we compute α^* from Equation (3) yielding:

$$\begin{array}{rl} \ell_u : & [lh, lt] \rightarrow [lt] \rightarrow [lt, rh] \rightarrow [lt, rh, rt] \\ \alpha^*(\ell_u) : & 46\% \rightarrow 19\% \rightarrow 18\% \rightarrow 17\%. \end{array}$$

We argue that if the objective is to obtain anthropomorphic bipedal walking, this optimal walking cycle should be matched as closely as possible. To demonstrate this, we use the optimal walking cycle to compute the HBC in several instances.

Humans. To quantify the differences in walking between the different subjects, we compute the HBC for each subject. The results of this computation are illustrated in Fig. 8. Interestingly, nearly all of the human walkers exhibit nearly uniform HBC and the uniformity of their cost is particularly striking.

Robots. Next, we use the HBC to compute the cost of walking for various bipedal robots without knee lock considered in the literature. Tlalolini et al. (2009) consider numerous bipedal modes with different numbers of domains (between 1 and 3) and walking gaits. We focus on two models that they present, one with cycle $\ell_2 : [lh, lt] \rightarrow [lt]$ and another with cycle $\ell_3^a : [lh, lt] \rightarrow [lt] \rightarrow [lt, rh, rt]$. Associated with these cycles, there are three walking cycles: $R_{2a} = (\alpha_{2a}, \ell_2)$, $R_{2b} = (\alpha_{2b}, \ell_2)$ and $R_{3a} = (\alpha_{3a}, \ell_3^a)$, for which the HBC is illustrated in Fig. 8. From the results of the computed HBC, we conclude that the model R_{3a} produces the most anthropomorphic walking as it has a dramatically lower cost than the other two models. In that paper the authors state that this walking cycle "is the closest to human gait" amongst the ones they consider, which the HBC agrees with.

Schaub et al. (2009) consider two bipedal walking gaits with a model consisting of cycle: $\ell_3^b : [lh, lt] \rightarrow [lt] \rightarrow [rh]$, where $[rh]$ is a domain not seen in human walking consisting of the bipeds only having one contact point at the right heel (a domain not found in human walking). Two walking cycles $R_{3b} = (\alpha_{3b}, \ell_3^b)$ and $R_{3c} = (\alpha_{3c}, \ell_3^b)$ are associated with this cycle for which the HBC can be computed; the result is illustrated in Fig. 8. Despite the fact that both of these models have three domains, they do not produce a HBC as low as walking cycle R_{2b} indicating that adding more domains does not necessarily result in more human-like walking.

6. CONCLUSION

In this paper, we resolve an outstanding debate within the bipedal walking community by showing that there exists a *universal* temporal ordering of events for bipedal walking. The human-based cost was then constructed to measure the anthropomorphism of gait. When the HBC was computed for existing bipedal walking robots, the robots with more "human-like" walking gaits were correctly identified. The results of this paper are also applicable to future bipedal robot design. If the universal domain breakdown is used for the robotic model, and the parameters of the controller used to achieve walking are chosen so as to minimize the HBC, the end result promises to be human-like walking.

REFERENCES

Ames, A., Vasudevan, R., and Bajcsy, R. (2011). Human-data based cost of bipedal robotic walking. In *Proceedings of the 14th International Conference on Hybrid Systems: Computation and Control*.

Ames, A.D., Gregg, R.D., and Spong, M.W. (2007). A geometric approach to three-dimensional hipped bipedal robotic walking. In *45th Conference on Decision and Control*. San Diago, CA.

Borgs, C., Chayes, J., Lovász, L., Sós, V., and Vesztergombi, K. (2008). Convergent sequences of dense graphs I: Subgraph frequencies, metric properties and testing. *Advances in Mathematics*, 219(6), 1801–1851.

Carlsson, G., Zomorodian, A., Collins, A., and Guibas, L. (2004). Persistence barcodes for shapes. In *Proceedings of the 2004 Eurographics/ACM SIGGRAPH symposium on Geometry processing*, 124–135. ACM New York, NY, USA.

Choi, J.H. and Grizzle, J.W. (2005). Planar bipedal walking with foot rotation. 4909–4916. Portland, OR.

Goswami, A., Thuilot, B., and Espiau, B. (1996). Compass-like biped robot part I : Stability and bifurcation of passive gaits. Rapport de recherche de l'INRIA.

Hatcher, A. (2002). *Algebraic Topology*. Cambridge University Press.

Schaub, T., Scheint, M., Sobotka, M., Seiberl, W., and Buss, M. (2009). Effects of compliant ankles on bipedal locomotion. In *IROS*. St. Louis, Missouri, USA.

Tedrake, R., Zhang, T., and Seung, H. (2005). Learning to walk in 20 minutes. In *Proceedings of the Fourteenth Yale Workshop on Adaptive and Learning Systems*. New Haven, Connecticut, USA.

Tlalolini, D., Chevallereau, C., and Aoustin, Y. (2009). Comparison of different gaits with rotation of the feet for planar biped. *Robotics and Autonomous Systems*, 57, 371–383.

Westervelt, E.R., Grizzle, J.W., Chevallereau, C., Choi, J., and Morris, B. (2007). *Feedback Control of Dynamic Bipedal Robot Locomotion*. Control and Automation. Boca Raton, FL.